ELSEVIER

Thin Solid Films 372 (2000) 212–217

thin solid films

www.elsevier.com/locate/tsf

Na in selenized Cu(In,Ga)Se_2 on Na-containing and Na-free glasses: distribution, grain structure, and device performances

A. Rockett[a,*], J.S. Britt[1,b], T. Gillespie[c], C. Marshall[c], M.M. Al Jassim[d], F. Hasoon[d], R. Matson[d], B. Basol[e]

[a] *1-107 ESB, University of Illinois, 1101 West Springfield Avenue, Urbana, IL 61801, USA*
[b] *Energy Photovoltaics Inc., P.O. Box 7456, Princeton, NJ 08543, USA*
[c] *Lockheed Martin Astronautics (LMA), P.O. Box 179, Denver, CO 80201, USA*
[d] *National Renewable Energy Laboratory, 1617 Cole Boulevard, Golden, CO, USA*
[e] *ISET Inc., 8635 Aviation Boulevard, Inglewood, CA 90301, USA*

Received 26 January 2000; received in revised form 8 May 2000; accepted 8 May 2000

Abstract

We examined the effect of deposition of Na on Mo-coated glasses and the Na content of the substrate glass on standard production Cu($In_{1-x}Ga_x$)Se_2 (CIGS)-based solar cells fabricated by selenization of Cu-Ga-In precursor thin films. Under optimal conditions, net Na content has a larger effect on the films than does the choice of substrate glass. Device performances improved with modest amounts of added Na on borosilicate glass. Device performances on soda-lime glass were not improved by adding Na. The supply of Na appears to have been adequate from the glass itself. A peak in device performance was found as a function of integrated Na in the CIGS layer as determined by secondary ion mass spectrometry (SIMS). The Na is found primarily in the areas of decreased grain size in the selenized CIGS where Ga is also found. S, deposited with the Na does not end up in the same place as does the Na. Rather, it tends to move toward the surface and accumulate in a buried layer. This is probably due to the reaction process rather than to the microstructure. Oxygen has no apparent effect on Na behavior in the CIGS.

Keywords: $CuInSe_2$; Photovoltaics; Thin Films; Sodium; Chalcogens; Selenides

1. Introduction

Production of large quantities of Cu($In_{1-x}Ga_x$)Se_2 (CIGS)-based solar cells (with $0 < x < 1$) requires a reproducible deposition process that reliably yields high quality material. To design and control such a process, it is of particular interest to know how process variables affect solar cell performance. Impurities, both beneficial and detrimental may be incorporated into the absorber layers during processing. CIGS-based devices deposited by evaporation have been found to show improvements in performance when Na is present during formation of the CIGS [1–10]. Most studies of device performance as a function of impurity content have focused on CIGS and Mo produced in the laboratory on small substrates. It is especially interesting to know how Na is incorporated into the CIGS absorber layers of solar cells produced by standard commercial techniques on soda-lime glass substrates and how it influences the properties of device-quality material.

Previous works have considered the effects of Na incorporated into polycrystalline CIGS layers grown by

* Corresponding author. Tel.: +1-217-333-0417; fax: +1-217-244-1631.
E-mail address: arocket@uiuc.edu (A. Rockett).
[1] Present address: Global Solar Energy, 5575 South Houghton Road, Tucson, AZ 85747, USA.

0040-6090/00/$ - see front matter
PII: S0040-6090(00)01028-2

multiple source evaporation [1,2,6–8], selenization [3–5,9], as well as in single crystal epitaxial layers [11]. These results have suggested that Na is incorporated in sputtered Mo. The Na resides primarily in the grain boundaries and does not move significantly in the grains of the Mo itself [12]. Further, it has been shown that the O concentration in the Mo plays a strong role in determining the Na content [12]. At least two groups have found evidence in the CIGS of enhanced grain growth, increased (112) texturing and an increase in device performance when Na was present in the films [2,3]. Another study indicated that Na decreases resistivity as well as the activation barrier to conduction in the plane of polycrystalline thin film CIS [4]. This behavior was attributed to a decrease in the potential barrier to conduction across grain boundaries. Still others have found that Na increases the open-circuit voltage of polycrystalline devices and reduces depletion width [1]. This may be linked to observed Na-induced reductions in compensation in CIS [11]. In a previous work, we studied the relationships among process conditions for several commercial Mo processes and Na incorporation in the Mo and pure CIS (no Ga) [13].

The current work examines the effect of deposition of Na on Mo-coated glasses and the Na content of the substrate glass on standard production CIGS fabricated by selenization methods. The work was performed as part of the CIS Team efforts coordinated by the National Renewable Energy Laboratory (NREL) through the Thin Film PV Partnership Program.

2. Experimental

The CIGS films used in this study were formed in the CIGS solar cell process line of Energy Photovoltaics (EPV). The procedures for deposition followed their standard method used to produce device-quality CIGS on Mo. A precursor consisting of layers containing Cu-Ga and In was deposited on a compound In, Ga selenide by evaporation. The precursors were heated to 400°C and exposed to a Se flux equivalent to a deposition rate of 3 nm s^{-1}. After a few minutes at 400°C, the desired amount of Na_2S was evaporated onto the CIGS film (see Table 1). The sample temperature was then ramped to 520°C for a short period of time. The layer was continually exposed to Se throughout the high temperature portions of the process. The film was allowed to cool naturally to room temperature. The amount of Na_2S listed below as added to the films is the estimated atomic percentage in the precursor films. This was determined to be approximately 12% of the Na_2S evaporated from the source. The relative amounts of Na actually incorporated into the final films depended upon the deposition conditions. The normalized integrated SIMS counts for Na in the various films are listed in Table 1. In all cases, samples on soda-lime glass had more Na in the final film than did the films on borosilicate glass. Even more Na could not be added to films as gross changes in CIGS film morphology began to occur for doses above the 3 at.% level.

Substrates consisted of Corning 7059 borosilicate glass coated with 1000 nm of Mo at Lockheed Martin Astronautics (LMA) or conventional soda-lime glass used in CIGS solar cell production coated with 500 nm Mo at EPV. The Mo deposition conditions were as follows. At LMA the magnetron power was 2 kW, the sputtering pressure was 9 mtorr, and the 1.2-mm-thick substrates passed by the magnetron twice. At EPV the magnetron power was 2 kW at a pressure of 10 mtorr. The glass samples passed by the magnetron twice.

Samples were analyzed by scanning electron microscopy (SEM) and grazing incidence X-ray diffraction (GIXRD) at the NREL. Secondary ion mass spectrometry (SIMS) in a Cameca IMS-5f instrument was carried out at the University of Illinois at Urbana-Champaign (UIUC). SIMS measurements used Cs^+ primary ion beams. Measurements of both positive and negative secondary ions were made in some cases although data presented below are for positive secondary ions. In addition, a few measurements were made using

Table 1
Na deposition doses, glass used and device performances

Sample	Cu/In + Ga	Na dose (At.%)	Na from SIMS (Arb. units)	V_{oc} (mV)	J_{sc} (mA cm^{-2})	FF (%)	Eff. (%)
Borosilicate glass							
6B	0.88	0	0.00003	396	35.8	57.9	8.2
1A2	0.90	0.06	0.0007	404	39.1	65.1	10.3
2A1	0.88	0.4	0.04	398	32.7	67.7	8.8
2A22	0.92	3	1	454	33.1	57.4	8.6
Soda-lime glass							
Comparable EPV device	0.9	0	0.1	459	37.0	69.1	11.7
2B2	0.89	0.06	0.5	475	39.6	70.5	13.2
3A2	0.88	0.4	0.1	433	35.1	67.4	10.2
2A2	0.90	3	3	350	34.1	49.3	5.9

O_2^+ ions when oxygen interferences or yield effects were suspected.

Standard ZnO/CdS/CIGS/Mo/glass solar cells were produced at EPV on pieces cut from the samples listed in Table 1. Each sample was dip-coated with CdS following a procedure described elsewhere [14]. ZnO was deposited by rf sputtering as a bilayer. The first (resistive) ZnO layer was ~50 nm thick and the second highly conductive layer was ~500 nm thick.

3. Results and discussion

CIGS films were produced on each of the Mo-coated glass substrates. The resulting layers were then cut into pieces and analyzed or used to produce solar cells. Cross-sectional SEM images of fractured CIGS/Mo/glass structures were obtained for each layer and selected images are shown in Fig. 1. Other images were generally similar. Adhesion of the films to the Mo back contacts varied with process conditions. Adhesion results were generally similar for both types of glass, although for a given Na level, the adhesion on the soda-lime glass was better than on the borosilicate glass. The worst adhesion was found for the samples with the highest Na level on both types of glass and was worst overall for sample 2A2 (~3 at.% Na, borosilicate glass). The sample without intentionally-added Na deposited on borosilicate (7059) glass showed excellent adhesion in a standard tape test. GIXRD was performed to determine the state of stress in layers 6B (no Na) and 2A1 (~0.4 at.% of Na) both deposited on borosilicate glass. No evidence of peak shifts was found, indicating that very high stress levels were not present in these films. In summary, the Na level had a larger effect on adhesion than did the type of substrate glass.

The microstructure of the films was observable from the cross-sectional SEM. The interface between the Mo and the CIGS is abrupt with no clear selenization of the Mo or penetration of the CIGS into the Mo observable, consistent with previous results [13]. Each CIGS film has a fine-grained (=0.1 μm) region extending through the rear half of the film. In addition, some of the images suggest a faint microstructure boundary at approximately one-quarter of the CIGS thickness below the surface. There is no obvious reason for a boundary at this point such as a pre-existing junction in the precursor layers. It is presumably a result of the complex reaction processes involved in selenization. There is no obvious correlation between the distinctness of this feature in the images and the composition of the films. The grain size in the top half of the CIGS layer was ~1 μm for ~0.06 at.% and ~0.4 at.% of Na added on both types of glass. At the highest Na level (~3 at.%) the grain size decreased rapidly yielding the most disorganized grain structure and the smallest grain sizes. As with adhesion, Na had a larger

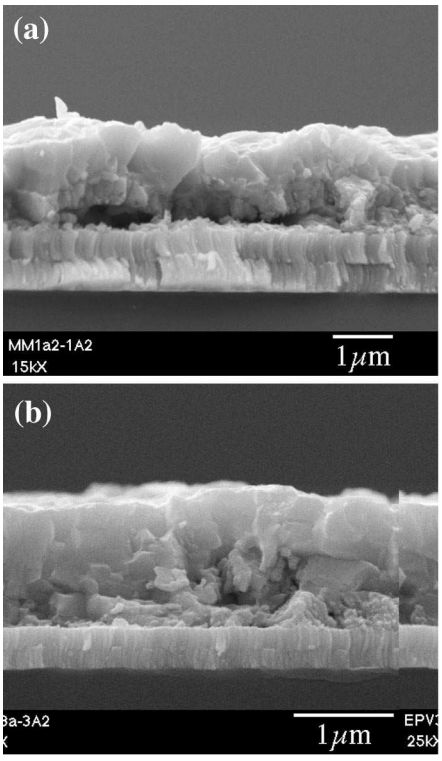

Fig. 1. Fracture cross-section scanning electron micrographs of (a) sample 1a2, CIGS deposited on LMA Mo on borosilicate glass with ~0.06 at.% Na, and (b) sample 3a2, CIGS deposited on EPV Mo on soda-lime glass with ~0.4 at.% of Na.

effect on film microstructure than did the type of substrate glass. Furthermore, the addition of Na did not improve the microstructure (increase grain size and uniformity) when beyond ~0.06 at.% of Na was added.

Typical SIMS results for the distribution of the major constituent elements of the CIGS and Mo films as well as the Na and oxygen distributions are shown in Fig. 2. The data shown are for CIGS deposited on Mo on soda-lime glass with ~0.4 at.% of Na. Fig. 3 shows profiles for S, O and Na for selected samples. Cu, In and Se signals are relatively constant throughout the thickness of the CIGS layers. Mo and Ga signals were all quite similar to those in Fig. 2. The samples show several distinguishable regions. The central regions of the films are relatively free of Ga, S and O. The Na signal in the central region is less than 10% of the value in the rear, Ga-containing region, or at the surface. The rear half of the samples contains effectively all of the Ga in a broad region. The rise in Ga concentration near the back of the selenized films is consistent with previous reports of Ga distribution in selenized CIGS. In the same area the Na and O signals rise.

The Mo signals increase reproducibly and consistently at the back of the CIGS suggesting that the CIGS/Mo interfaces are equivalent and abrupt as indicated by the cross-sectional SEM images. The Mo

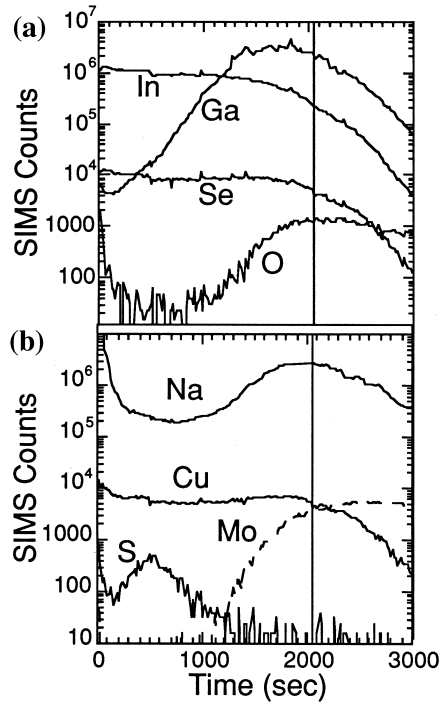

Fig. 2. SIMS depth profile data for sample 3a2. The minimum oxygen signal is a factor of 20 above the SIMS background.

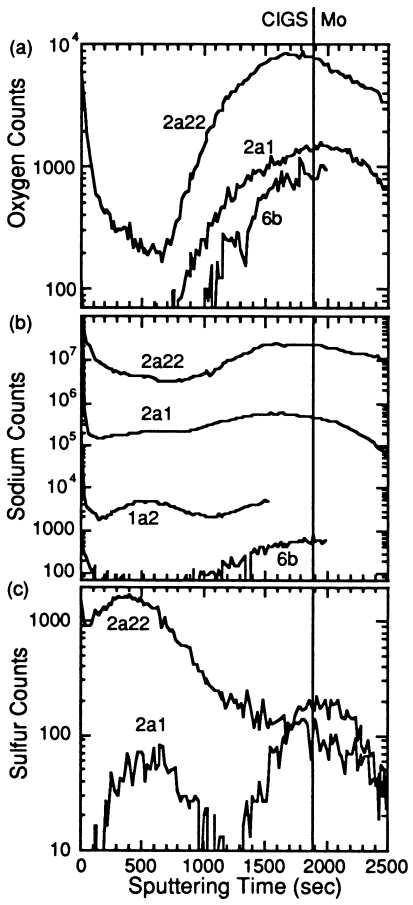

Fig. 3. Plots of depth profiles for (a) O, (b) Na and (c) S for selected samples as labeled. Oxygen profiles for samples 1a2, 3a2 and 2b2 were similar to the 2a1 profile shown. S profiles showed no signal in the CIGS for samples 1a2 and 6b. The 3a2 S profile was similar to that for 2a1 (see Fig. 2). Profiles for sample 2a2 were similar to those for 2a22 for all three elements.

signal increase rate thus indicates the depth resolution of the SIMS profiles. Because the Ga, O and Na signals rise at essentially the same rate as the Mo signals (but closer to the surface), it is likely that the transition from the Ga-poor to the Ga-rich region is also quite abrupt. This agrees with the cross-sectional SEM data. At the same depth where Ga increases, a large rise in grain boundary density occurs quite abruptly (see discussion above).

The ratio of Na and Ga signals over the region in which the Ga occurs is relatively constant for a given sample. The value of this ratio increases with increasing Na level from film to film. The ratio is also higher for films on soda-lime glass than it is on borosilicate glass for a given Na precursor dose. Apparently, sufficient Na supply is important in establishing the ratio value. However, the source of the correspondence between Na and Ga concentrations is not clear. The increase in Na is probably due to an increase in grain boundary volume rather than directly due to an increase in Ga. The effect of grain boundary volume may explain the lower Na/Ga ratio near the peak of the Ga for the film with ~ 0.4 at.% Na compared with the film with ~ 0.06 at.%. This film has somewhat larger grains in general. A direct chemical link between the Ga and Na contents seems unlikely. Analysis of epitaxial layers with large variations in Ga concentration and no grain boundaries showed no evidence of variation in Na concentration. Furthermore, SIMS analysis of polycrystalline samples formed by evaporation does not show an obvious correlation between Ga and Na. It should be noted that because selenization is such a different process chemically from evaporation, it is possible that Ga affects Na in selenization in ways not relevant to evaporation methods. As previously observed [13]. the Mo deposition process (i.e. deposition at LMA or EPV) had no apparent effect on the above results.

It can be argued that the Na level is related to changes in the O content. It is true that the general shape of the O, Na and Ga profiles are very similar. However, the SIMS data indicate that the O level varies by only a factor of ~ 10 from film to film, while the Na level changes by many orders of magnitude. There is virtually no Na in film 6B (10^{-6} times that in film 2A2), deposited without intentional addition of Na, while there is a large amount of Na in the two films dosed to ~ 3 at.% Na. By comparison, there is only a modest change (a factor of 10) in oxygen in the same films. Near the film surface, the O and Na signals drop rapidly into the sample as surface contamination is

removed. This is typical of SIMS analyses of all samples and in this region it is likely that O and Na signals are connected and related to establishment of the profiling. Where oxygen increases concurrently with Na it is probably a measure of the increasing grain boundary area, rather than a direct connection of the two elements to each other existing, in agreement with a previous study [9]. If it was the case that Na and oxygen were directly linked, then large increases in overall oxygen level should have occurred when large changes in overall Na resulted.

The above data suggest that Na increases near the rear of the films primarily because of increases grain boundary volume which, in turn, result from the reaction process. At the same time, this process drives Ga to the high grain-boundary density areas. The level of Na is then determined by the amount of Na available at the start of selenization either from the substrate or from the Na_2S dose. Apparently, the Na does not increase grain size in the Ga-rich region in selenization processes as much as it does in some evaporated materials. The level of Ga and O may have some effect on Na level but if so the relationship is not obvious.

The most significant chemical feature in the top half of the CIGS films is a peak in the S concentration. This reaches a maximum at approximately one-quarter of the thickness of the CIGS layer below the surface and falls off both toward the surface and toward the bulk of the CIGS layer. The peak in the S is not correlated with increases in any other element. However, the peak occurs at the same location as a weak change in microstructure observed by cross-sectional SEM. No significant increase in S is observed where grain size decreases toward the back of the films. Thus, there is no direct relationship between S and grain size. The amount of S found in the samples is strongly related to the dose of Na_2S provided to the sample. This is not surprising, as the Na_2S is the only significant source of S available during film growth. We conclude that S accumulated near the front of these selenized films because of the selenization process kinetics and the evolution of different phases in the material during selenization. We expect that any relationship of S to the microstructure is coincidental or due to the location of an intermediate phase during reaction.

Devices were tested in EPVs solar simulator and the

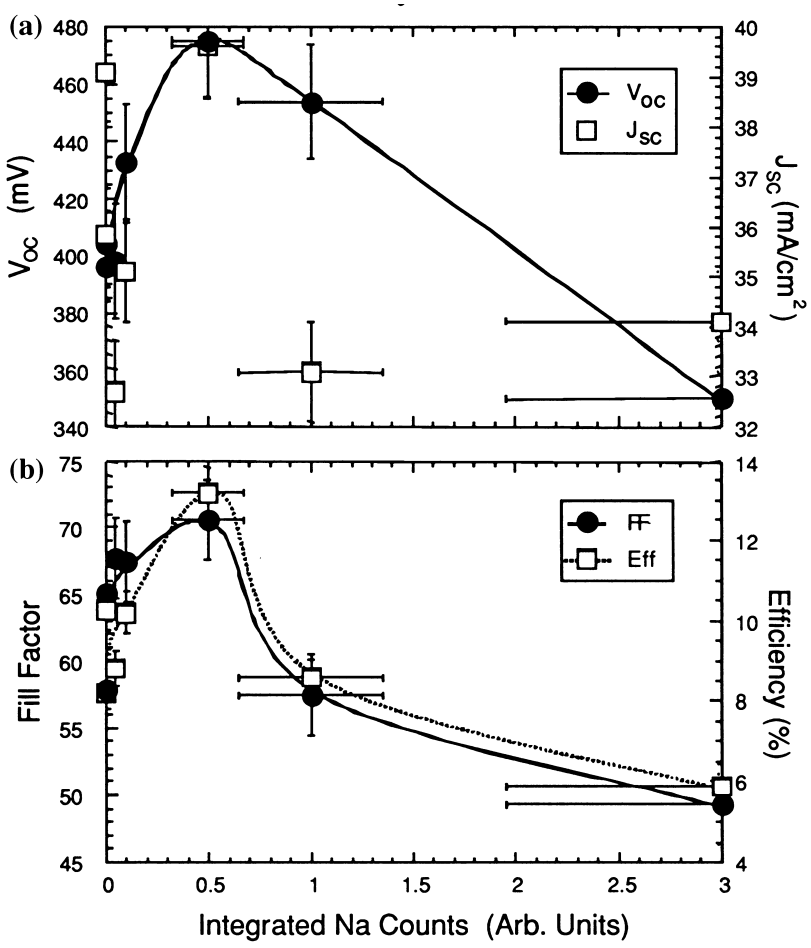

Fig. 4. Solar cell performance variables as a function of Na content as measured in the device layers by SIMS. Error bars are estimated based on typical SIMS analysis errors, examination of the SIMS data in question, and typical variations in solar cell device performances.

performance data are given in Table 1. The data suggest that added Na has an optimum concentration, see Fig. 4, for all normal solar cell parameters except J_{sc}. Because SIMS is not adequately quantitative and because the levels are non-uniform and below easy detection by energy-dispersive spectroscopy (EDS), we are unable to identify the optimal Na concentration specifically. The optimum value for addition of Na for samples on soda-lime glass is small or zero, indicating that adequate or nearly adequate Na is supplied from the substrate.

4. Conclusions

Several overall conclusions can be drawn from this work concerning CIGS formed by selenization processes. First, net Na concentration has a larger effect on the films than does the choice of substrate glass. Device performances improved with modest amounts of added Na on borosilicate glass. Device performances on soda-lime glass were not improved by adding Na. The supply of Na was adequate from the glass itself. Large amounts of Na were detrimental to device performances. These conclusions are in general agreement with previous results (see, e.g. [6–8]). The Na is found primarily in the areas of selenized CIGS where grain boundary density is highest. Increased Ga and O are also found in these areas. The increase in Ga is probably due to the reaction process while the increased O is presumably related to larger grain boundary volume. The O increase is smaller than that of Na in these areas and the two are not obviously correlated other than through the grain boundary volume. S, deposited with the Na does not end up in the same area as does the Na. Rather, it tends to move toward the surface and accumulate in a buried layer. This is probably due to the reaction process rather than to the microstructure.

Acknowledgements

The authors gratefully acknowledge the support of the National Renewable Energy Laboratory under the Thin Film PV Partnership and Universities programs. The advice and comments of the other members of the CIS team are also appreciated. A. Rockett also acknowledges the support of the Electric Power Research Institute and the Department of Energy under contract DEFG02-91ER45439. Lockheed Martin Astronautics (LMA) participation was funded by combined LMA Internal Research and Development Project D90D, Advanced Structures, Materials and Controls, and under Defense Advanced Research Project Agency (DARPA) Agreement MDA972-95-3-0036, Vapor Phase Manufacturing of Thin Film Flexible CIS Photovoltaics.

References

[1] M. Ruckh, D. Schmid, M. Kaiser, R. Schäffler, T. Walter, H.W. Schock, Proceedings of the First World Conference on Photovoltaic Energy Conversion, Waikoloa, HI, USA, December 5–9, 1994, (1994) 156.
[2] M. Bodegård, L. Stolt, J. Hedström, in: R. Hill, W. Palz, P. Helm (Eds.), Proceedings of the 12th European Photovoltaic Solar Energy Conference, Amsterdam, Netherlands, April, 1994, (1994) p. 1743.
[3] V. Probst, J. Rimmasch, W. Riedl et al., Proceedings of the First World Conference on Photovoltaic Energy Conversion, Waikoloa, HI, USA, December 5–9, 1994, ((1994)) 144.
[4] J. Holz, F. Karg, H. von Philipsborn, in: R. Hill, W. Palz, P. Helm (Eds.), Proceedings of the 12th European Photovoltaic Solar Energy Conference, Amsterdam, Netherlands, April, 1994, (1994) p. 1592.
[5] U. Rau, M. Schmitt, D. Hilburger, F. Engelhardt, O. Seifert, J. Parisi, Proceedings of the 25th IEEE Photovoltaic Specialists Conference, Washington, DC, USA, May 13–17, 1996, (1996) 1005.
[6] J.E. Granata, J.R. Sites, S. Asher, R.J. Matson, Proceedings of the 26th IEEE Photovoltaic Specialists Conference, Anaheim, CA, USA, September 29–October 3, (1997) 387.
[7] J.E. Granata, J.R. Sites, in: J. Schmidt (Ed.), Proceedings of the Second World Conference on Photovoltaic Energy Conversion, Vienna, Austria, July, 1998, (1998) p. 604.
[8] R.J. Matson, J.E. Granata, S.E. Asher, M.R. Young, in: M. Al-Jassim, J.P. Thornton, J.M. Gee (Eds.), Proceedings of the 15th NCPV Photovoltaics Program Review, American Institute of Physics Conference Proceedings, 462, (1998) p. 542.
[9] J.H. Scofield, S. Asher, D. Albin et al., Proceedings of the First World Conference on Photovoltaic Energy Conversion, Waikoloa, HI, USA, December 5–9, 1994, (1994) 164.
[10] S. Zweigart, S.M. Sun, G. Bilger, H.W. Schock, Solar Energy Mater. Solar Cells 41 (2) (1996) 219.
[11] D.J. Schroeder, A.A. Rockett, J. Appl. Phys. 82 (1997) 4982.
[12] K. Granath, L. Stolt, M. Bodegård, A. Rockett, D.J. Schroeder, in: H.A. Ossenbrink, F. Helm, H. Ehmann (Eds.), Proceedings of the 14th European Photovoltaic Solar Energy Conference, Barcelona, June 30–July 4, 1997, (1997) p. 1278.
[13] A. Rockett, K. Granath, S. Asher et al., Solar Energy Mater. Solar Cells 59 (1999) 255.
[14] J. Britt, C. Ferekides, Appl. Phys. Lett. 62 (22) (1993) 2851.